University of Washington
AIAA Design, Build, Fly 2012-2013
Design Report

DawgAir 313

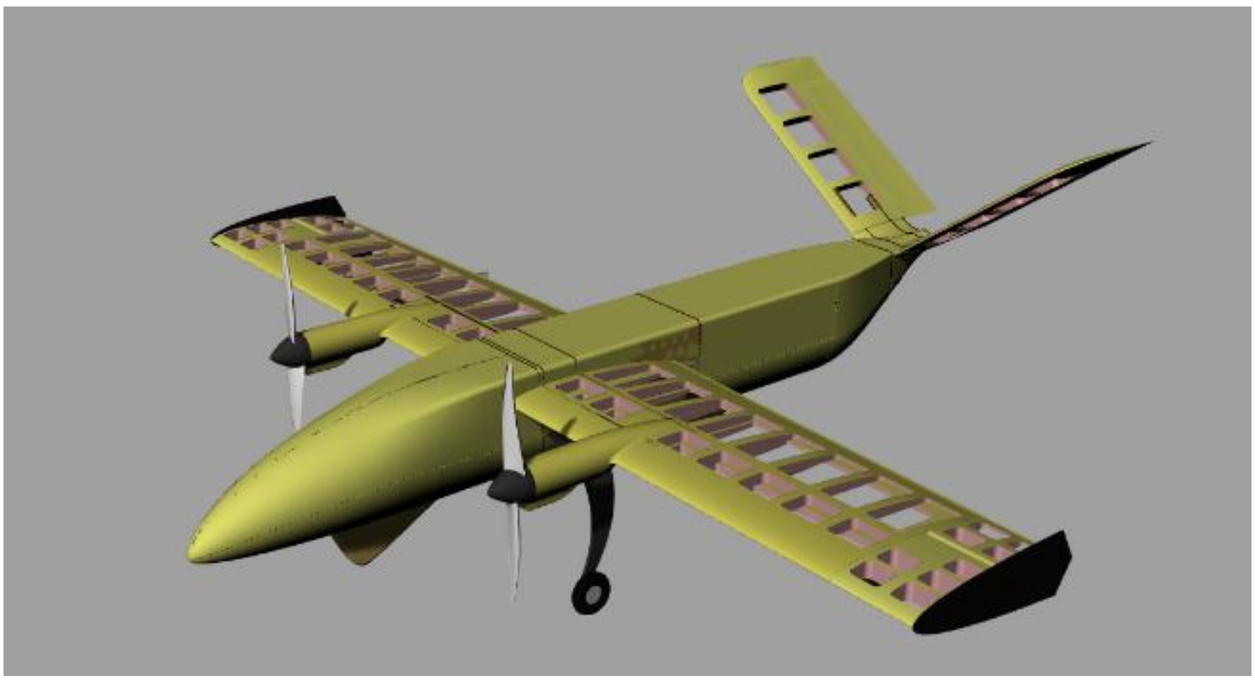

TABLE OF CONTENTS

NOMENCLATURE

EW	empty weight [lbs]
C_{HT}	chord of horizontal tail
C_m	coefficient of moment
L_{HT}	moment arm from wing-body center of gravity to tail aerodynamic center
N_{laps}	number of laps completed
$N_{max\ l}$	maximum number of laps completed
N_{stores}	number of rockets carried
$N_{max,s}$	maximum number of rockets carried
RAC	rated aircraft cost
SF	size factor [ft]
S_{HT}	horizontal tail area [in^2]
S_{VT}	vertical tail area [in^2]
S_{VTAIL}	total area of V-tail [in^2]
T	time to complete Mission 3 [s]
T_{min}	minimum time to complete Mission 3 [s]
α	angle of attack [degrees]
δ	mathematical operator – partial derivative
γ	dihedral [degrees]

1. EXECUTIVE SUMMARY

The design submitted by the University of Washington for the 2012-13 AIAA DBF competition was based on two factors: mission requirements and feasibility of design. To begin, attention was turned towards existing aircraft whose missions align with the outline of the competition; these included both heavy lift aircraft to account for the payload, light utility aircraft for short take-off and low stall speed characteristics, and pylon racing aircraft for performance when on the flight course. With these aircraft in mind, the design was tailored to the exact mission requirements set forth in the competition rules.

The missions for this competition simulate a highly maneuverable, highly versatile aircraft, whose performance specifications fall within the regime of that of military operations; specifically those of the joint-strike fighter. With a short distance take-off included with each mission, the aircraft had to be designed to maximize power output under various loading conditions without requiring excessive structural support. With two missions tailored to high performance take-offs, the difficulty of the design was increased with the additional requirement of the aircraft to complete as many laps as possible through the flight course in a set time.

As the takeoff distance was the most challenging aspect of the competition, many of the design considerations and efforts were concentrated here. To address this issue, design elements were considered from both heavy-lift high-performance transport military aircraft, such as the Boeing C-17 Globemaster III, as well as light general aviation aircraft, such as the Piper Cub J3. From the C-17, the general shape of the fuselage, as well as the high wing placement was taken. High wings were considered as having the main structural support for the wings placed at the top of the fuselage would maximize the amount of area within the fuselage to place the payload. Likewise, the idea of utilizing high-lift devices was taken from the C-17 in the form of near full-wing flaps. From the Piper Cub, the idea of using conventional landing gear was taken to place the wings at a set angle of incidence when on that ground that would allow for optimum lift with minimal drag during takeoff.

To address the speed mission, a pylon racing airfoil was chosen to allow for minimal drag characteristics. In addition, larger pitch propellers were chosen to be used on the speed mission to increase the top speed of the aircraft.

The initial design of the aircraft included the use of Styrofoam construction to decrease the total weight of the plane. Through wind tunnel testing, it was found that structurally, the Styrofoam was inadequate, and thus the design was changed to incorporate carbon fiber within the fuselage as well as on the wings and tail.

The final design of the aircraft incorporated a high wing design with a 95% flap to allow for a short take-off with a slow stall speed. In its loaded configuration with a maximum estimated payload of 3.5 pounds, the aircraft is designed to weigh approximately 9 pounds. The maximum speed of the aircraft is estimated to be around 60 mph, allowing the completion of around 6 laps during the first mission. The approximate take-off distance of the aircraft is 25 feet at a takeoff speed of 30 feet per second. As such, the aircraft meets the minimum performance requirements necessary to complete the competition.

2. MANAGEMENT SUMMARY

2.1 Design Team Organization

The University of Washington's 2012-2013 Design, Build, Fly (DBF) Team consists of 14 dedicated students, not all-exclusive to the Department of Aeronautics and Astronautics. Displayed in Fig. 2.1 is merely an outline, as all team members contribute to each group to complete milestones, communicate progress, and promote new ideas.

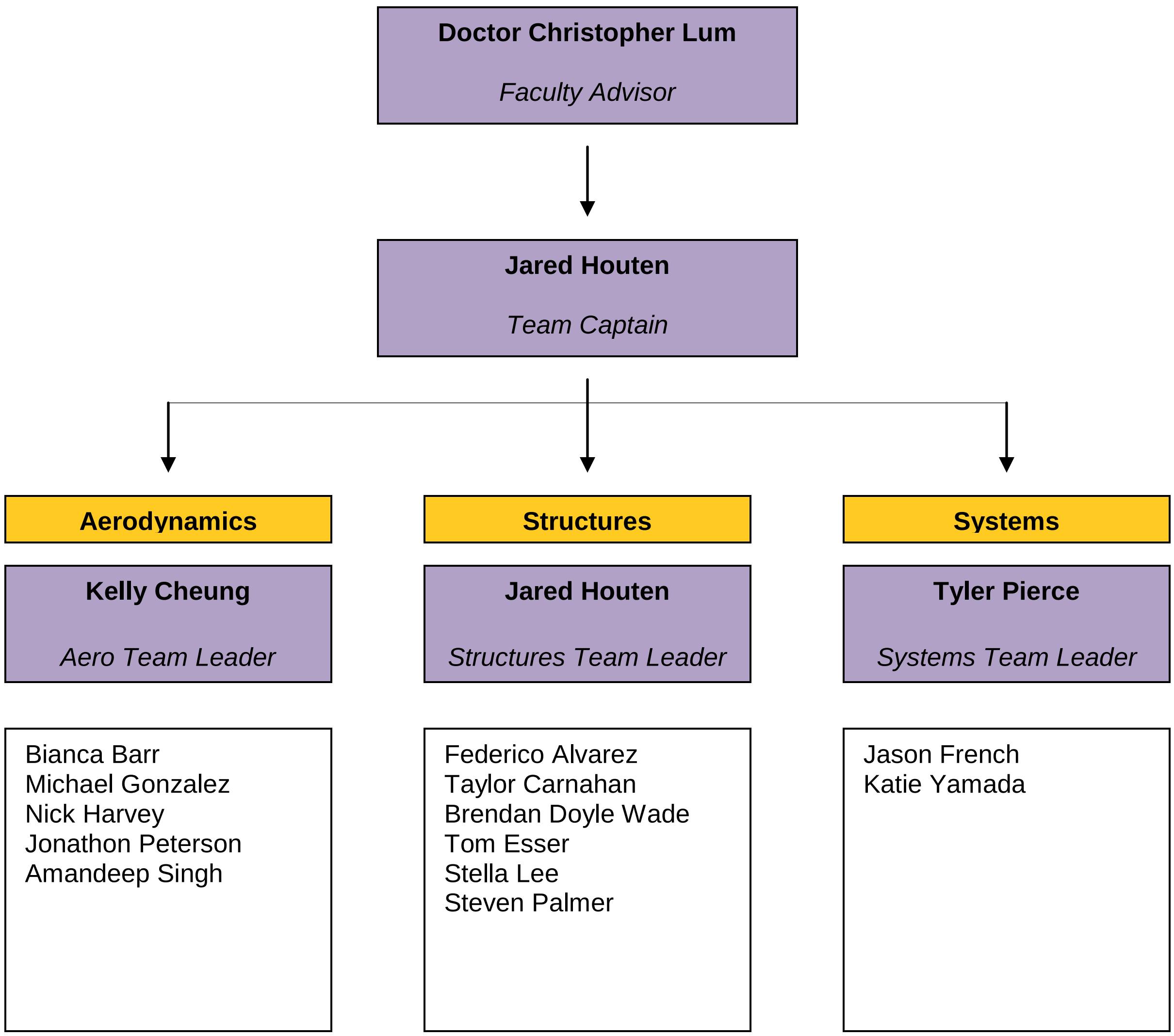

Figure 2.1. Team organization chart.

The team is divided into three teams: Aerodynamics, Structures, and Systems. The team captain is in charge of overseeing the progress of each team, managing the budget, and steers the progress of the overall team. Each team has a leader that is in charge of team gatherings, directing workflow, and communicating with the other team leads. The Aerodynamics team is in charge of the overall design of the aircraft and all the aircraft's flight surfaces, as well as conducting the wind tunnel tests of the complete model. The Structures team constructs the aircraft and chooses the most suitable methods and materials to do so. They are also in charge of structure tests that test the model's ability to endure the range of loads that will possibly be imparted to the aircraft, and creating the SolidWorks drawings. The Systems team is responsible for choosing and appropriately integrating the optimal batteries, motors, and controls.

2.2 Project Design Schedule

The team had 7 months to prepare for the competition in April. Within these 7 months, the team was able to design, construct, and test the prototype. After analyzing the results of the tests of the prototype, the final aircraft was designed and constructed. In Fig. 2.2, the project design schedule is displayed. This design schedule allowed for any possible fine-tuning and optimization of the aircraft, as well as allowing time for the pilot to become familiarized with the aircraft.

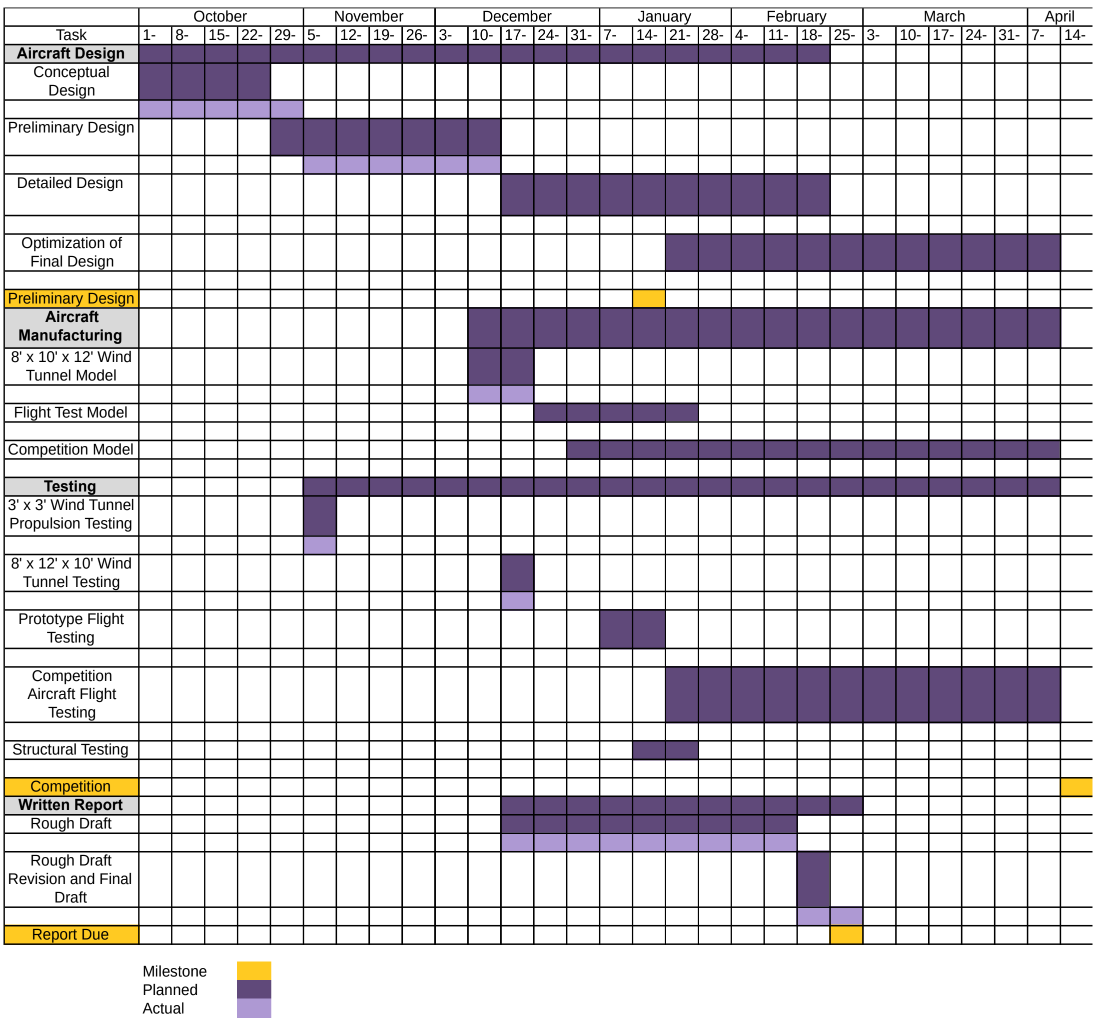

Figure 2.2. Project design schedule.

3. CONCEPTUAL DESIGN

During the conceptual design phase, the contest rules provided on the 2012-2013 AIAA DBF website were analyzed to create a set of criteria that the aircraft must satisfy. This set of criteria, or design goals, was then considered during the trade study to determine the configuration of the aircraft. Certain design goals were highlighted and prioritized, which led to an aircraft that would perform well in all of the missions and yield the highest overall score.

3.1 Competition Requirements and Rules

The requirements for all aircraft entering in the 2012-2013 AIAA DBF competition are listed below [1]:

- Commercially available and electrically powered propeller.
- Maximum current drawn from the battery pack(s) or received by the motor(s) limited to 20 Amps.
- Maximum battery pack(s) weight of 1.5 pounds.
    - Must use over-the-counter NiCad or NiMH batteries.
- Secure payloads so center of gravity does not have significant variation during flight.
- Aircraft's wing structure must be able to endure entire aircraft weight when supported at wingtips.
- Unassisted takeoff within a 30 x 30 foot square.

The competition's flight course is displayed in Fig. 3.1.

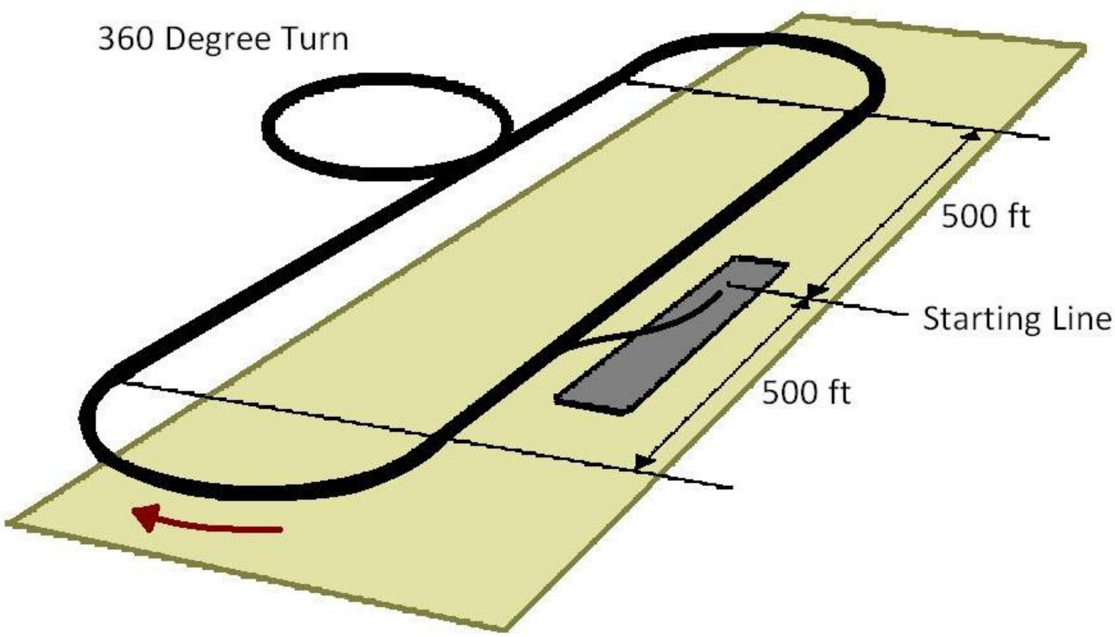

Figure 3.1. Flight Course.

3.2 Mission Objectives

The missions this year focus on aircraft performance, with emphasis on:

- Short takeoff.
- High top speed.
- Payload ratio.
- Aircraft stability, balance; and maneuverability.

The mission objectives of and scoring criteria for each mission are detailed in the following subsections.

3.2.1. Short Takeoff

The first mission requires the aircraft to take off within a 30 x 30 foot marked square and complete as many laps of the circuit as possible within 4 minutes. In order to complete the mission, the aircraft must land successfully. The Mission 1 (M1) score is dependent upon the number of laps completed, N_{laps}.

$$M1 = 2 * \left(\frac{N_{laps}}{N_{\max,l}}\right) \qquad \text{Eq. (3.1)}$$

3.2.2. Stealth Mission

The second mission tests the payload ratio of the aircraft. For Mission 2 (M2), the payload is the maximum amount of Mini-Max rockets that the aircraft is designed to carry within its fuselage. This amount must not be zero and cannot exceed the amount present during the tech inspection. After completing the short takeoff, the aircraft must complete 3 laps with the internal stores. The number of rockets held by the aircraft, N_{stores}, determines the M2 score.

$$M2 = 4 * \left(\frac{N_{stores}}{N_{\max,s}}\right) \qquad \text{Eq. (3.2)}$$

3.2.3. Strike Mission

The third and final mission focuses on the aircraft's stability and balance by testing the aircraft's ability to withstand different variations of payload configurations. These payloads are combinations of different rockets at different locations on the aircraft. The combination to be flown for the mission is determined by rolling a die. After installation of the payload, the aircraft must take off within the square and fly 3 timed laps. The Mission 3 (M3) score is subject to the time flown for the mixed-stores flight, *T*.

$$M3 = 6 * \left(\frac{T}{T_{min}}\right) \qquad \text{Eq. (3.3)}$$

The total score that the team will receive depends on the score received on the written report, the sum of the scores received for each mission, and the rated aircraft cost (RAC). Incorporated into the RAC are the empty weights measured after each successful scoring flight, *EW*, and the size factor, *SF*. *SF* is dependent upon the wingspan and overall length of the airplane.

$$Total\ Competition\ Score = Written\ Report\ Score * \left(\frac{Total\ Flight\ Score}{RAC}\right) \quad \text{Eq. (3.4)}$$

Where the Total Flight Score is determined by:

$$Total\ Flight\ Score = M1 + M2 + M3 \quad \text{Eq. (3.5)}$$

The RAC is determined by:

$$RAC = \frac{\sqrt{EW * SF}}{10} \quad \text{Eq. (3.6)}$$

The SF is determined by:

$$SF = x_{max} + 2 * (y_{\max}) \quad \text{Eq. (3.7)}$$

Where x_{max} is the wingspan and is the wingspan and y_{max} is the total length of the aircraft, from nose to tail. Finally, the EW is determined by:

$$E = Max\ Empty\ Weight\ (M1, M2, M3) \quad \text{Eq. (3.8)}$$

3.3 Design Requirements

A low empty weight is necessary for all three missions, though each individual mission has certain additional design requirements in order to receive the highest possible score for that particular mission. These requirements are listed below for each mission.

Mission 1: Maximum Lap Flight

To successfully complete this mission, the aircraft must be fast and maneuverable. The aircraft will not be carrying any loads, so the necessary cruise lift coefficient will be low due to the light aircraft. The aircraft must have high aerodynamic efficiency and the propulsion system must be capable of outputting power at low and high speeds. The aircraft must also be capable of generating the high lift necessary for a short takeoff.

Mission 2: Maximum Internal Store Flight

This mission requires a spacious fuselage that will hold as many internal stores as possible while minimizing drag. The configuration of the stores must be in a way that promotes an aerodynamic design of the aircraft while allowing suitable separation between each store. Short takeoff is again a major mission obstacle.

Mission 3: Unknown Stores

This mission requires the aircraft be capable of carrying a multitude of possible store combinations. This introduces many design complications, because the wing must have load bearing hard points designed into it, and the stability characteristics of the aircraft could change dramatically depending on the payload.

When these design requirements are combined, a diametrically opposed set of airplane characteristics is created. The two main contradictions, creating high lift while maintaining high top speed and maneuverability, and minimizing overall dimensions while maximizing gross payload, presented a very difficult design challenge. The team discussed which characteristics were most important, which would result in greater points overall, and based the final design decisions on these characteristics. An analysis of the scoring method revealed that reducing aircraft weight would have the greatest effect on the overall score, allowing for smaller wings and increasing the overall speed of the aircraft. After weight, the number of stores flown in the second mission would have the next greatest effect on the total score. It became apparent that the ideal aircraft for this competition was lightweight and fast, but could carry many internal stores.

3.4 Configuration Selection

To determine the optimum configuration for the aircraft, different features of the aircraft were considered and compared. For a thorough trade study, the pros and cons of each component were deliberated and rated. These were ranked relative to the most conventional configuration by a negative or positive integer respectively, with the conventional configuration set to 0 as the baseline. A higher integer indicates the amount of weight that a pro or con carries for the configuration. This rating criterion was taken from each team's standpoint to encourage discussion on how each configuration is viewed by each team, and the reason for each rating is given in their respective tables. The five aspects of the conceptual design that were considered were the wing and wing mounting, landing gear, propulsion, and empennage. The fuselage size and shape would be determined based on the number of rockets carried, a decision process which is discussed in a later section.

3.4.1. Wing Selection

For basic wing design, the team conducted a trade study to decide which configuration would suit the mission of the aircraft best. Table 3.1 shows the result of the trade study, using the mono wing as the control in which compare all other wings to.

Table 3.1. Wing Selection.

	Aerodynamics	Structures	Systems	Total
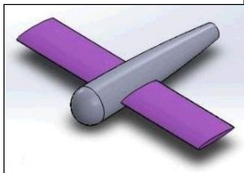 **Mono-wing**	0	0	0	**0**
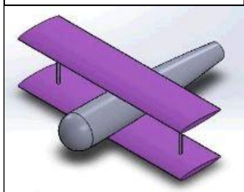 **Biplane**	+1. Extra lift. -2. More drag.	+1. Decreased wingspan. -1. Extra bracing. -1. 2 wings to build. -2. Ground clearance.	-1. Extra servos/linkages.	**-5**
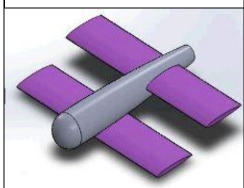 **Tandem Wing**	+1. More options for external payload. -1. Less maneuverable. -1. Less efficient.	+1. Decreased wingspan. -1. Extra bracing. -1. 2 wings to build.	-1. Extra servos/linkages.	**-3**
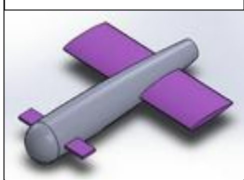 **Canard**	+1. Favorable stall characteristics. -2. Decreased maneuverability. -1. Less efficient. -1. Stability issues.	0	0	**-3**
 **Flying Wing**	+1. Least drag. -3. Less stability.	+2. Simpler, continuous construction. -2. Ground clearance. -2. Internal payload shape not optimal.	+1. Fewer servos. -4. Significant control challenge.	**-7**
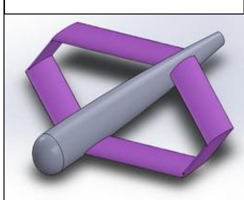 **Box Wing**	+1. Less lift-induced drag. -1. Less efficient.	+1. Decreased wingspan. -1. Extra bracing.	-1. Extra servos/linkages. -1. Possible control challenge.	**-2**

As displayed and reasoned in Table 3.1, the chosen wing for this year's aircraft is the mono-wing. Despite the larger dimensions for the same wing area, the mono wing provided the best flight characteristics and the simplest construction. The team decided the wing would be mounted high on the fuselage, due to the external payload that will need to be mounted beneath the wing. This also provided clearance for propellers.

3.4.2. Landing Gear Selection

Landing gear selection was limited in design to those that would be fixed to the aircraft, as actuators or mechanisms would overcomplicate the aircraft and compromise space. Table 3.2 shows the trade study conducted on landing gear.

Table 3.2. Landing Gear Selection.

	Aerodynamics	**Structures**	**Systems**	**Total**
 **Conventional (Taildragger)**	0	0	0	**0**
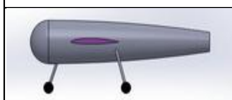 **Tricycle Gear**	-1. More drag.	-1. More support structure needed, less room for stores.	0	**-2**

According to Table 3.2, this year's aircraft was designed to have conventional landing gear.

3.4.3. Propulsion Selection

Propulsion selection was based on the number of propellers desired to propel the aircraft and their orientation. For practicality the team chose between one or two propellers in either a push or pull configuration. Table 3.3 shows the results.

Table 3.3. Propulsion Selection.

	Aerodynamics	Structures	Systems	Total
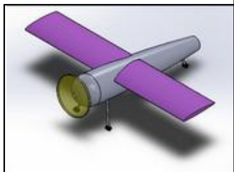 **Single Engine**	0	0	0	**0**
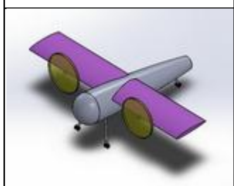 **Twin Engine**	+1. Improved airflow over wing on takeoff. +1. Less torque effect.	+3. Non-centered engine frees space in fuselage for payload. +1. Less ground clearance needed for smaller props. -1. Stronger wings needed.	+1. More power. -1. Additional wiring. -1. Additional weight. -1. Less efficient.	**+3**
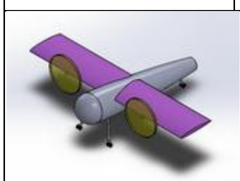 **Pull Prop**	0	0	0	**0**
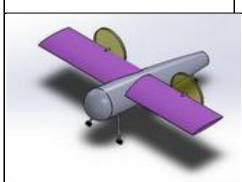 **Push Prop**	-2. Decreases efficiency of props. -1. Less stable. -1. Worse weight distribution.	-1. Ground clearance for props on takeoff.	-1. Decreased cooling.	**-6**

A twin engine, puller prop configuration was decided upon for the aircraft. This was ideal for maximizing internal payload volume while minimizing overall size. It also provided favorable behavior on takeoff, and minimized ground clearance necessary for the props.

3.4.4. Empennage Selection

Selection of the tail follows the same trend as other aspects of the aircraft with the conventional crucifix tail as the control. The result of team discussion is displayed in table 3.4.

Table 3.4. Empennage Selection.

	Aerodynamics	Structures	Systems	Total
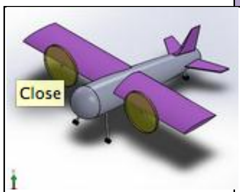 **Conventional**	0	0	0	**0**
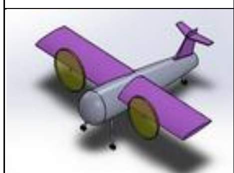 **T-Tail**	+1. Horizontal tail is more efficient.	-2. Construction challenge.	-1. Difficulty with servo placement.	**-2**
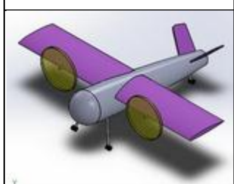 **V-Tail**	+1. Less drag.	+1. Easier to build.	0	**+2**

The V-tail offers several advantages over the conventional tail. Chief among these is that the V-tail accomplishes the same control authority for less total surface area. This means that the tail will generate less drag and weigh less relative to the conventional tail, while offering the same flight characteristics. The control mixing for the V-tail is accomplished in the transmitter, and does not require modifying the onboard electronics. The V-tail is also easier to build and integrate with the fuselage, as there are fewer surfaces to join.

3.4.5. Payload Arrangement and Fuselage Shape

The requirement of carrying internal stores necessitates another close examination of the scoring equation. The minimum number of rockets that can be carried internally is 4, and the maximum is 14. Clearly, there is a tradeoff between the number of rockets carried and the size and weight of the airplane, but it was found that the increases in size were quantized relative to increasing the number of rockets. This was because of the way that the team decided to fit the rockets inside the fuselage, which is illustrated in the figure below.

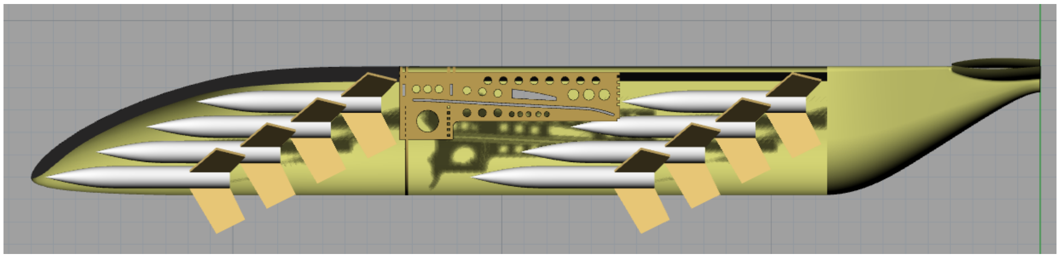

Fig. 3.2. Rocket layout within fuselage.

It was decided that building the fuselage to carry 8 rockets offered a good compromise between size and carrying capacity, and did not substantially increase the weight over carrying just 4 rockets. No change in main fuselage architecture was needed, only an increase in the length of the longitudinal supports. This also meant that the difference in size was limited to the length dimension, which carries half the point penalty of the width dimension. The fuselage also incorporates room for electronics and batteries, whose location was not determined until after the aerodynamic stability characteristics were experimentally defined.

3.5 Wing Design

One of the distinguishing features of this year's competition is the short take off requirement. This significantly influenced the design of the aircraft, and led to the creation of the key feature of our airplane, the morphing wing. This wing is characterized by a flap that runs 95% of the chord, 50% of the thickness, and 80% of the span of the wing. When this flap is not deployed, the airfoil of the wing is symmetric, promoting high speed and maneuverability, as well as docile stall characteristics. With the flap deployed, the wing area nearly doubles, and the cross section of the wing airfoil changes to that of a highly cambered lifting shape. This promotes short take off capability and allows for a decrease in the wingspan needed for takeoff. This morphing wing creates two drastically different flight characters that were determined to be necessary to succeed in the competition, and also helps keep exterior dimensions to a minimum.

4. PRELIMINARY DESIGN

The purpose of the preliminary design process was to establish the initial dimensions of the craft. It was necessary to closely analyze the attributes of many different features, and consider their impact on the total system performance. This section will explain the reasons for configuration sizing choices, and demonstrate the decision process utilized in establishing the maximum performance configuration.

4.1 Design Analysis and Methodology

The process began with a close examination of the various degrees of freedom of the airplane design within the chosen configuration constraints. Fuselage size, propulsive power, wing size, tail size, payload weight, and overall weight were evaluated from a design perspective. The assumptions made were validated in the wind tunnel, and the airplane design was tuned based on the results of the test.

4.2 Design and Sizing

4.2.1 Wing Sizing

The minimum takeoff distance imposes a significant limitation on the aircraft design. Because power output is limited, the takeoff distance is directly proportional to the weight and wing area of the aircraft. The heavier the load, the bigger the wing must be to achieve liftoff in a 30’ square box. The overall takeoff weight became the first evaluative obstacle. Assumptions had to be made about the weight of craft and the weight of the payload, even though no detailed design had been done. These estimates were based on a takeoff velocity calculated using an iterative method in MATLAB. This calculation accounted for changing lift, drag, and power during the take off roll. Difficulty was encountered in calculating an accurate available power curve because of unknown motor performance and propeller efficiency. Because these assumptions would motivate the entire design, it was decided that a power test should be performed. This was conducted in the University of Washington 3’ x 3’ Low Speed Wind Tunnel. A motor and prop were chosen based on previous experience, and were mounted on a six-component force transducer, as shown below. The power came from a DC power supply, and an optical tachometer was used to measure RPM so that prop efficiency could be determined. The tunnel was run at an array of wind speeds designed to envelop the predicted flight regime, and thrust and power output were measured at each speed.

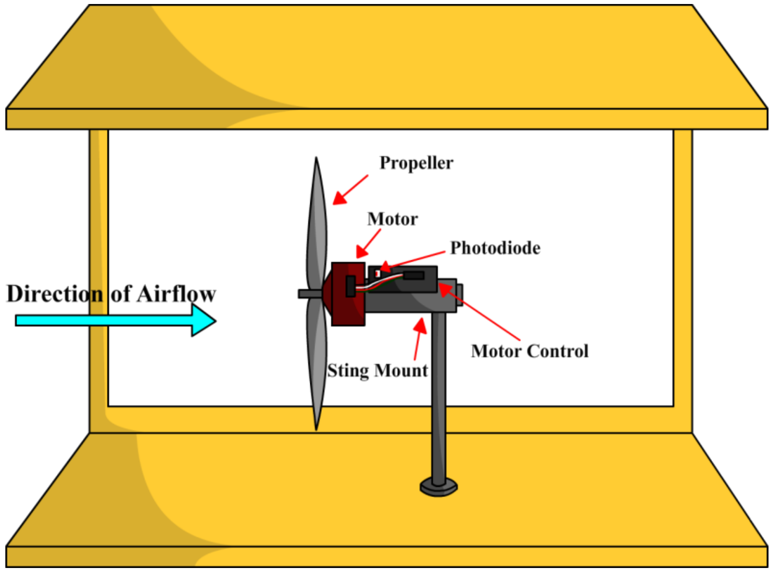

Fig. 4.1. Power testing of propeller and motor to determine power available for take-off roll

Based on the results of the power test, it was found that a top speed of 30ft/s could be reached within the takeoff box. After figuring out this number, a variety of airfoils were examined to see which ones would provide optimal performance and necessary lift for the smallest total wing area. It was found that for an assumed mass payload fraction of 55%, a Martin Hepperle 25 pylon racing airfoil would be ideal for producing the lift needed in cruise. The shape of the takeoff airfoil was determined by the structural requirements for the flap section, and closely resembles an Eppler 423 Low Reynolds Number airfoil. Each wing in cruise configuration was designed to have a total area of 250in^2. The maximum flap size that was possible within that wing was determined to be 150in^2. This meant that the total wing area with the flaps deployed would increase 300in^2, for a total takeoff wing area of 800in^2.

4.3 Wing Design

After the establishment of initial aircraft dimensions, a wind tunnel test was needed to verify the aerodynamic performance of the design. A model was constructed out of high-density insulation foam and carbon fiber spars, and mounted in the Kirsten Wind Tunnel at the University of Washington Aeronautical Laboratory. The purposes of the test were to explore the performance characteristics of the wing and establish the geometry of the flight surfaces relative to the fuselage. Because wing performance was not yet known, the test was conducted without tail surfaces. Following the test, a tail was designed to provide the control authority that the data indicated was needed. The optimum angle of incidence of the wing was determined, as well as the deployment position of the flap. The behavior of the airplane at many different attitudes was tested, and the stability characteristics were experimentally verified. The proximity of the Kirsten Wind Tunnel and ease of testing offered an excellent alternative to exhaustive computer simulation, and provided very accurate and reliable design information. Shown below are images of the test setup.

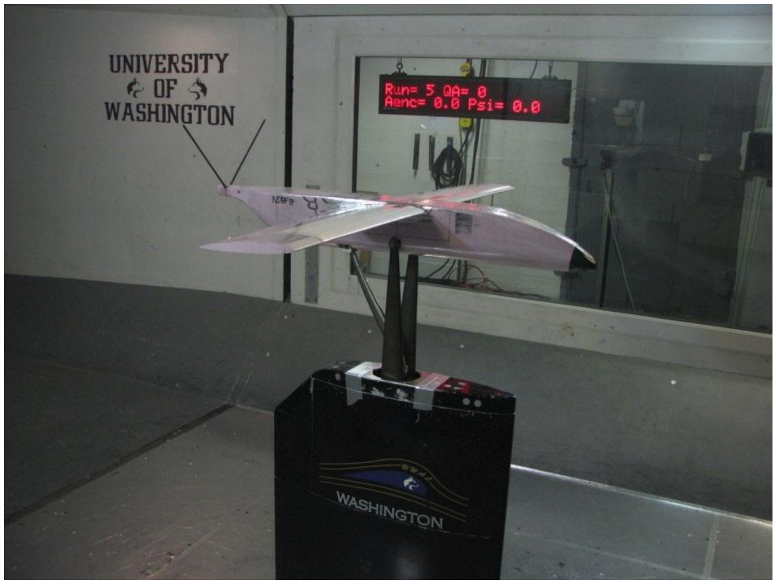

Fig. 4.2. Model mounted in the KWT test section.

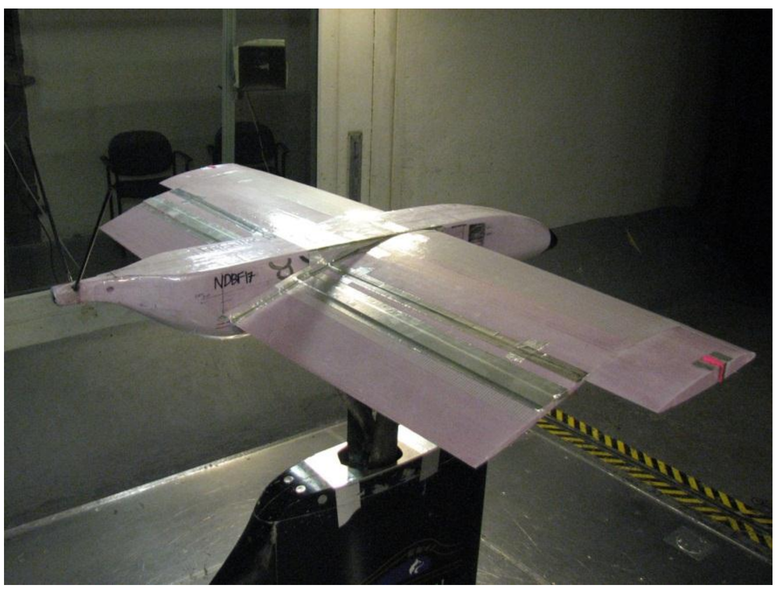

Fig. 4.3. Model with flap section deployed.

The angle of incidence of the cruise wing relative to the fuselage (4°) was determined by finding the angle at which the lift generated by the wing was equal to the lift needed for straight level cruise flight. The various angles tested are shown below in Fig. 4.4.

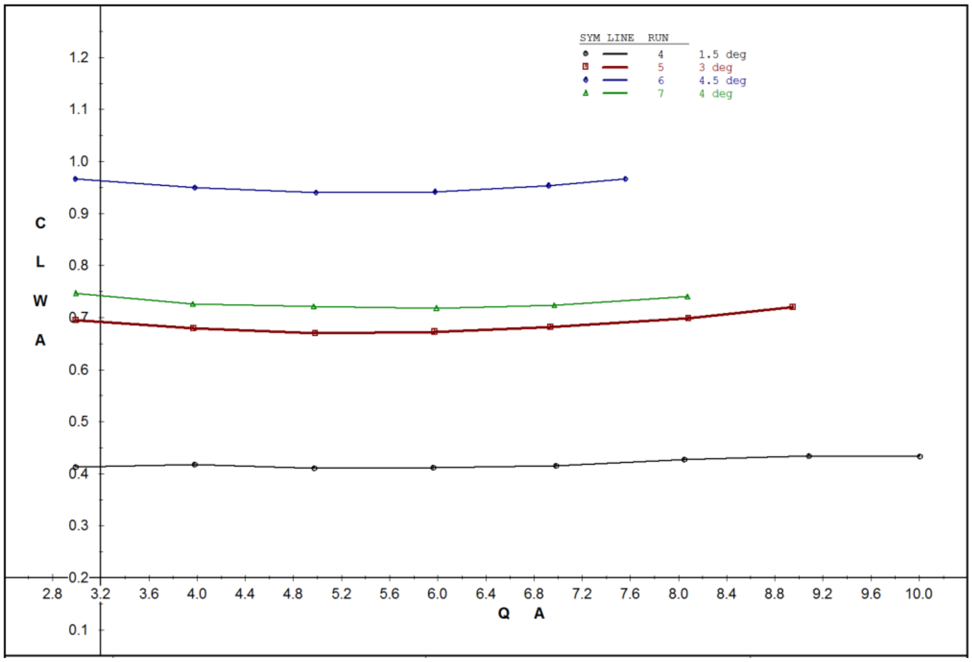

Fig. 4.4. Lift coefficient vs. dynamic pressure for varying angles of incidence of the cruise wing.

The flap angle of incidence of 12° was chosen to balance maximum lift and pitching moment, shown in Fig. 4.5

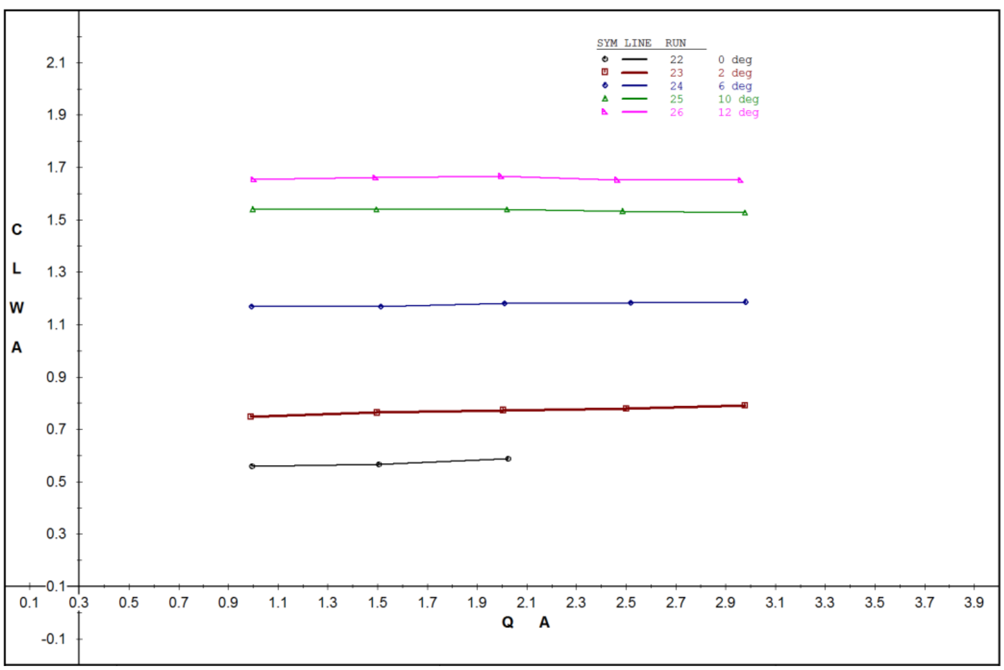

Fig. 4.5. Lift coefficient vs. dynamic pressure for varying angles of incidence of the takeoff flap.

The lift slopes of the airplane in takeoff and cruise configurations are shown in Fig. 4.6 below.

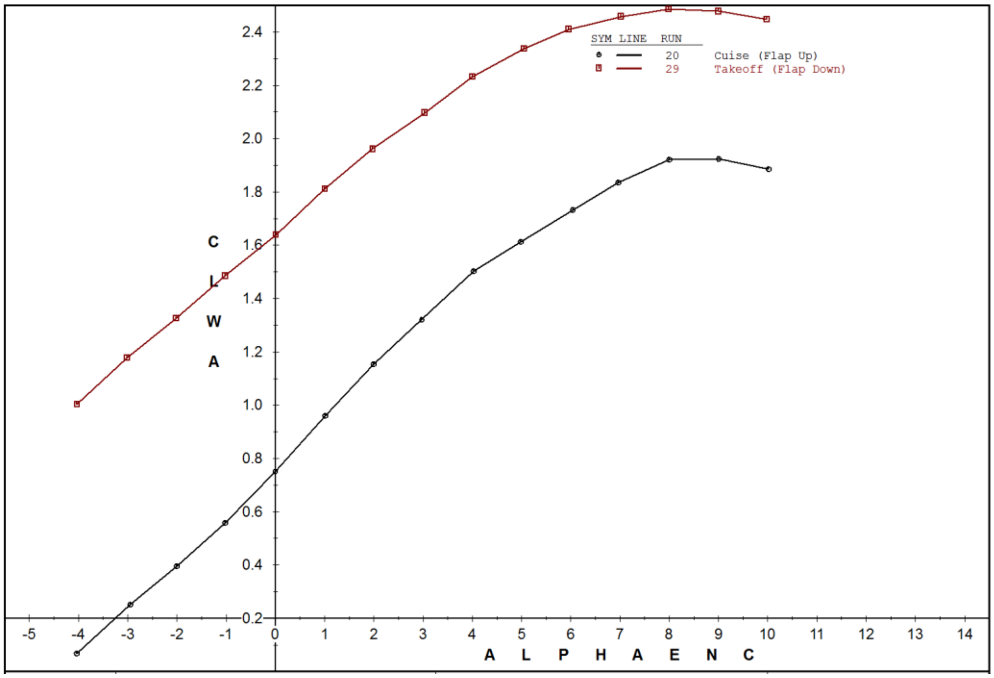

Fig. 4.6. Lift coefficient vs. angle of attack for cruise and takeoff wing configurations.

The drag polar plots for each wing configuration are shown below.

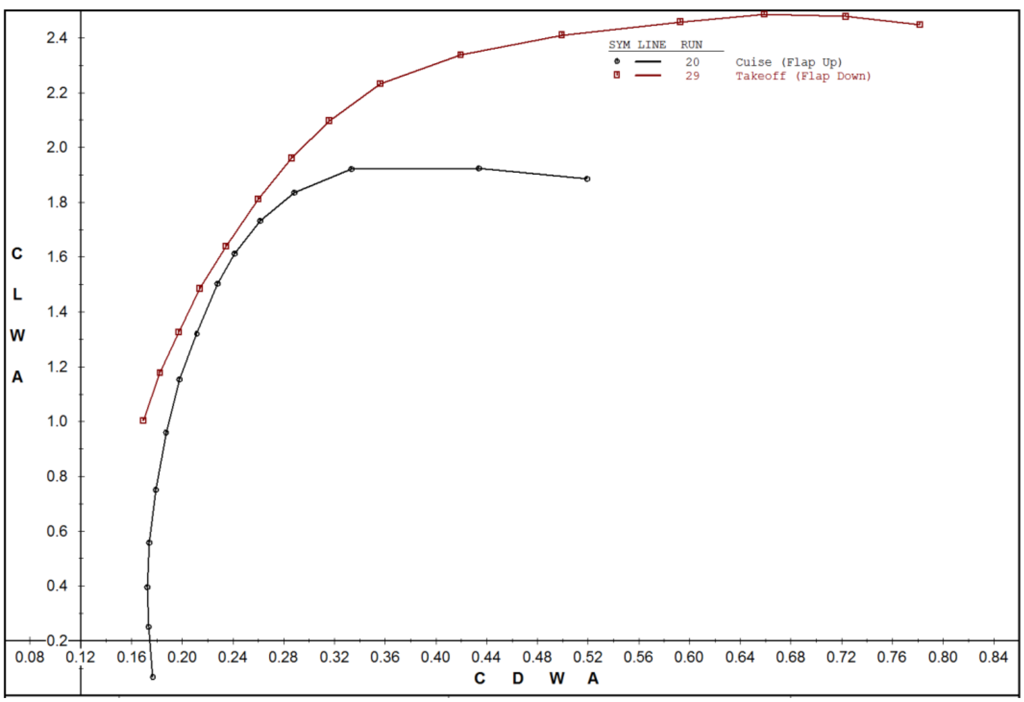

Fig. 4.7. Lift coefficient vs. drag coefficient for cruise and takeoff wing configurations.

The pitching moment plots for each wing are shown below.

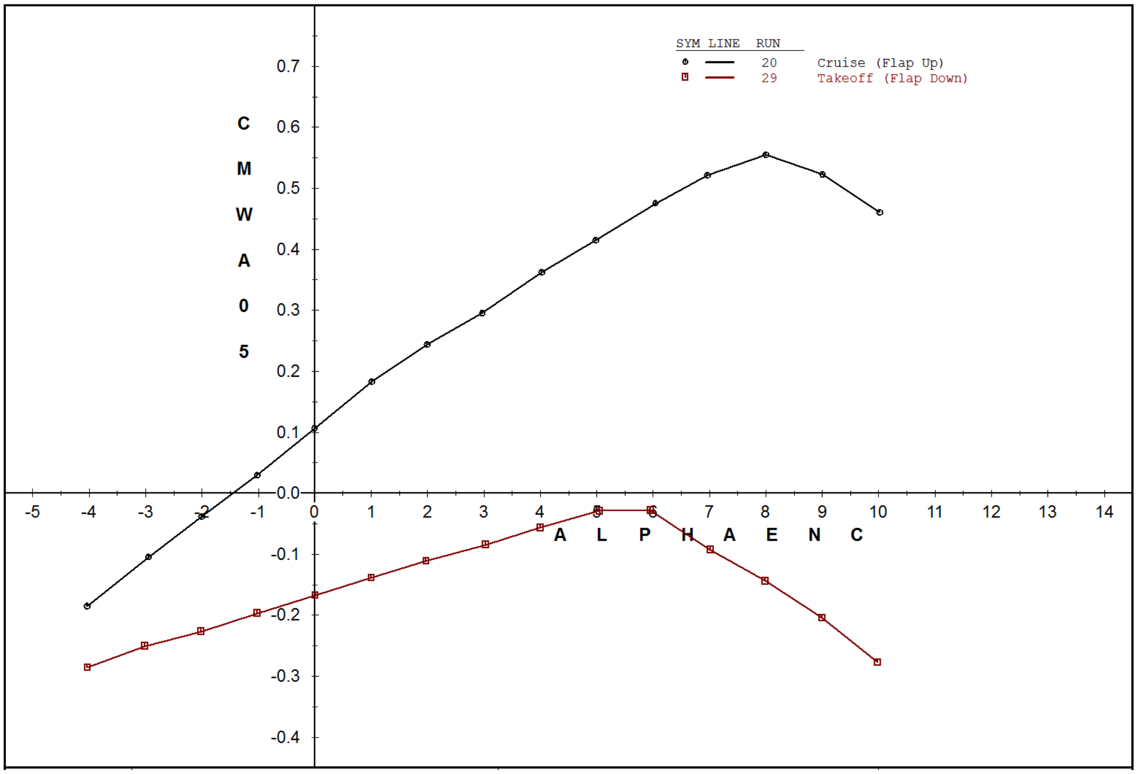

Fig. 4.8. Pitching moment vs. angle of attack for cruise and takeoff wing configurations.

The pitching moment slopes above are characteristic of the model without tail surfaces. This means that the performance of the wing could be studied as a singular entity, and the tail could be designed to provide exactly the effect needed to ensure stability.

The flap was tested with and without a gap, and the data plots are shown below in Fig. 4.9.

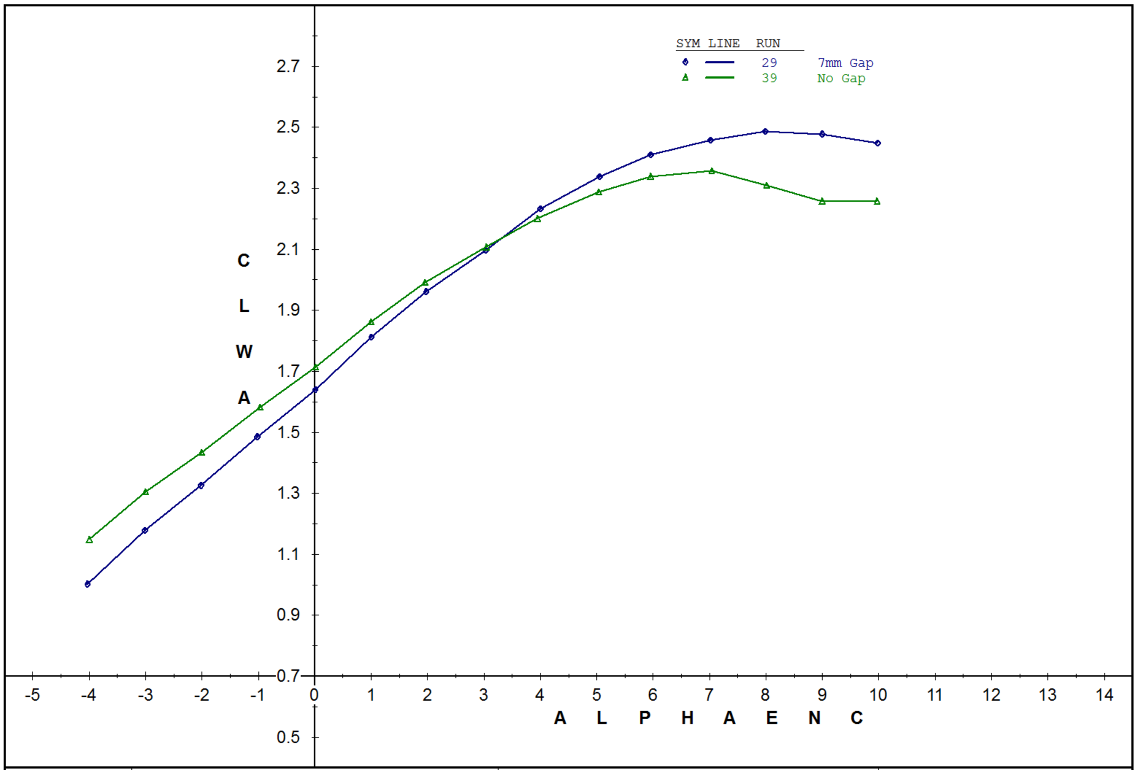

Fig. 4.9. Lift coefficient vs. angle of attack for flap with and without gap.

Note that the flap with a gap has a greater maximum lift coefficient and delayed onset of stall. The stall is also much more benign in character. For these reasons, a gap of 7mm was chosen for the final flap deployment position.

A vital piece of information gleaned from the wind tunnel test was the change in lift center of the aircraft. Because the aerodynamic behavior varies so drastically from takeoff to cruise configuration, maintaining longitudinal stability became a serious design concern. It was important to learn the effect of the flap on the dynamics of the craft, and this was achieved after the test using the data reduction software at the wind tunnel. Five virtual moment centers were chosen along the body of the craft, near the wing root. Force and moment data was computed for each of these points. Of particular interest in determining longitudinal stability characteristics is the change in pitching moment with respect to the angle of attack. By computing this slope at each of the five moment centers and interpolating between the points, the location where the slope was equal to zero was determined. This point corresponded to the aerodynamic force center of the wing. By constructing these plots for each wing configuration and finding the difference in the zero slope locations, the change in the aerodynamic center between the two wing shapes was determined. This plot is shown in Fig. 4.10.

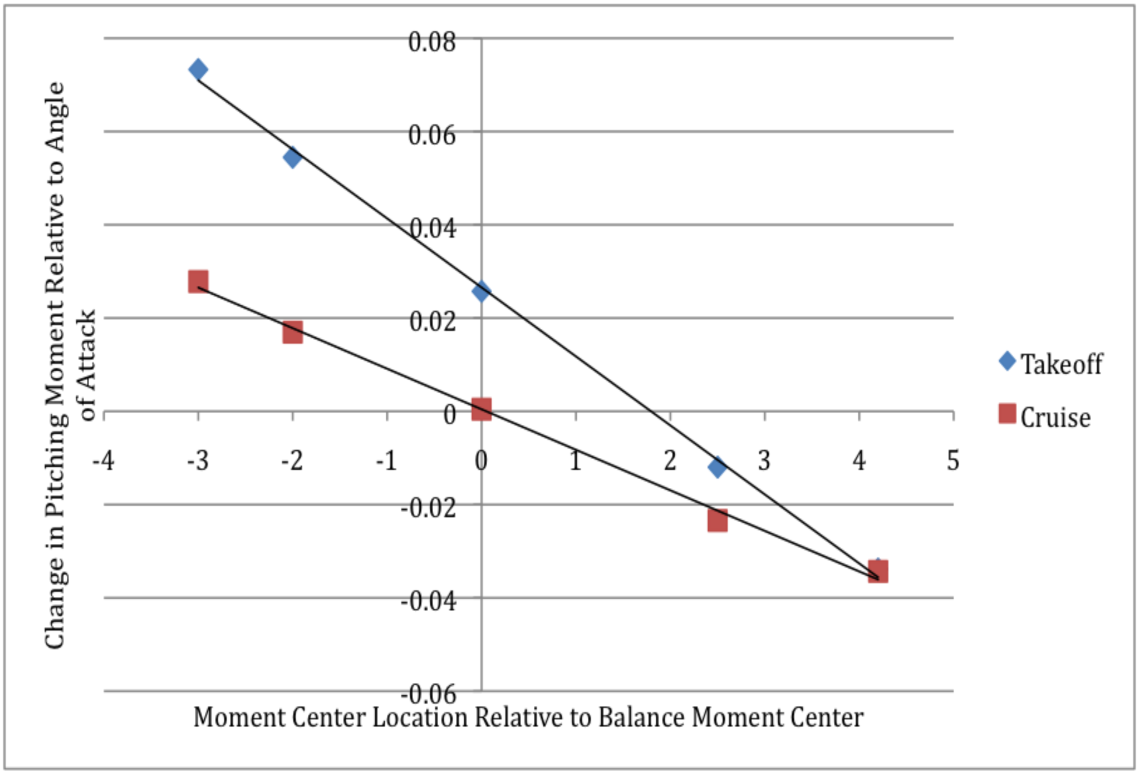

Fig. 4.10. $\frac{\partial C_m}{\partial \alpha}$ vs. distance from balance moment center.

As can be seen above, the aerodynamic force center of the wing changes roughly 1.8” between cruise and takeoff configurations. In order to maintain controllability, it was decided that the center of gravity of the aircraft should be located at the aerodynamic center of the wing in cruise configuration, to impart a neutral handling character in cruise mode. When the wing is in takeoff mode, the airplane will be more stable. Based on this test data, final choices regarding wing size, tail size, center of gravity location, and internal structure design were made.

4.3.1. Tail Sizing

For initial sizing, the stability of the aircraft had to be considered. As a V-tail design was chosen, the areas to consider for all stability calculations corresponded to the projected areas into the vertical and horizontal planes. The tail volume coefficient method was used [2]:

$$S_{HT} = \frac{c_{HT} * wing\ span * wing\ area}{L_{HT}}$$

The horizontal tail volume coefficient, c_{HT}, was estimated to be 0.6 for an RC aircraft with higher wing loading. S_{HT} represents the horizontal tail surface area. L_{HT} is estimated as the distance between the wing and tail quarter chords. L_{HT} was picked to be approximately 24 inches and S_{HT} was found accordingly. Using S_{HT} and choosing the tail's angle (γ) from the horizontal to be 35°, the vertical tail surface area (S_{VT}) was found:

$$S_{VT} = \tan(\gamma)^2 \, S_{HT}$$

which gives the total V-tail surface area [2]:

$$S_{VTAIL} = S_{HT} + S_{VT}$$

It was decided that the tail would not be tapered to simplify construction. Finally, the aspect ratio was chosen to be 3.5 based on geometry, the selected dihedral, and other aircraft tail ratios. This allowed the calculation of the chord. The tail sizing values are given below.

Table 4.1. Tail Dimensions chosen for the aircraft

Tail Dimensions	
V-Tail total wetted area	2.31 ft^2
Angle from horizontal (dihedral)	35°
Tail moment arm (¼ chord of wing to ¼ chord of tail)	25.5 in
Aspect Ratio	1.78
Tail chord	7 in

4.4 Mission Model

4.4.1. Mission 1

- Lift off within the prescribed area.
- Fly as quickly as possible around the course within the time limit.
- Land successfully.

Based on the lift generated in the wind tunnel test, the unloaded craft should easily be able to lift off within the 30' by 30' box. The power available as well as the variable wing shape should allow for very quick flight through the course.

4.4.2. Mission 2

- Load internal stores.
- Lift off within the prescribed area.
- Fly three laps.
- Land successfully.

The carrying capacity of 8 rockets is a good compromise between cargo capacity and aircraft size. As discussed earlier, the size of the aircraft must change to accommodate more rockets, which reduces score. The chosen cargo size represents a large amount of cargo, using the variable wing shape to lift off within the prescribed area.

4.4.3. Mission 3

- Load random assortment of stores.
- Lift off within the prescribed area.
- Fly 3 laps within the shortest possible time.
- Land successfully.

Base on lift and power available as discovered throughout wind tunnel testing, the aircraft will be able to take off and perform this mission quickly, as it is designed to carry more weight than that of any of the combinations of cargo loads.

5. DETAIL DESIGN

As the aircraft was physically constructed, problems and design issues that were not previously addressed became apparent. This section details the further optimization of the aircraft design statistics as well as some specific characteristics that were not discussed in the preliminary design. These changes will be embodied in the flight test model of the aircraft.

5.1 Dimensional Parameters

Detailed dimensions for the aircraft are given in Tables 5.1 through 5.4

Table 5.1. General Dimensions and Capacity

Airplane dimensions	
Length	48 in
Span	53 in
Height	5.75 in
Mission 1 weight	4 lbs
Mission 2 weight	6 lbs
Mission 3 weight	7.5 lbs

Table 5.2. Detailed Wing Dimensions

Main wing	
Airfoil	MH25
Cruise Area	500 in^2
Takeoff Area	800 in^2
Aileron Area	15.7 in^2
Flaps	156 in^2

Table 5.3. Detailed Tail Dimensions

Tail	
Airfoil	S1048
Span	12.5 in per panel
Chord	7 in
Dihedral	35°
Area	2.31 in^2
Aspect ratio	1.8

Table 5.4. Detailed Propulsion Parameters

Propulsion	
Motor	2 x KD A22-20L 1000kv
Gear ratio	1:1
Batteries	Elite 1500 (2 x 5 cell pack)
Propellers	11 x 5.5 & 10 x 7

5.2 Structural Characteristics

The scoring analysis shows that a decrease in weight and increase in speed have the largest impact on the total score. Since weight is directly correlated to speed, the team strived for the lightest possible airplane.

All materials chosen are of high strength to density ratio. Composite materials such as carbon fibers, epoxy resin, fiberglass, and Kevlar fabrics were all thoroughly investigated. The final aircraft took advantage of properties of multiple materials such as lightweight foam, plywood sheeting, and molded fiberglass and carbon fiber.

5.3. Systems and sub-systems design, component selection, integration and architecture

5.3.1. Structures

Main wing flap section – The inboard 20 inches of each wing corresponding to the location of the flap was made using a carbon layup technique onto light-weight insulating foam. Each foam core was wire-cut using steel stencils in the shape of the desired airfoil. Within the foam structure of the wing are two carbon spars running back into the superstructure within the fuselage. The carbon sheeting was placed atop the foam in the fashion of a veneer. With the foam interior and the rigid carbon exterior, the foam acts to absorb the shear stresses within the wing while the carbon fiber structures, both the spars and the veneer, absorb the normal stresses, including the tensile and compressive stresses do to wing flexure under loading. This resulted in an effective and efficient load transfer by the carbon fiber components into the fuselage superstructure while still maintaining efficient use of the foam core.

Outer wing section – The outer section of the wing corresponds to the aileron section. This section was made using the same carbon layup technique onto light-weight insulating foam. Instead of wire-cutting this section, the foam was milled using a foam CNC machine. As the aileron section would not be subjected to loading aside from the aerodynamic forces seen as a function it moving through the air, the foam section was milled with a series of cavities within it. The aileron itself was also milled from the aileron section core, allowing for precision mating surfaces between the static outer wing section and the aileron. Again, this section, the aileron and the static outer wing section, were both laminated using carbon fiber.

Tail – The tail section was made similar to the outer wing section. The core of each tail panel was milled within the foam CNC machine and subsequently laminated with carbon fiber. Within the foam core was placed a carbon spar to act as both a stiffening agent, designed to carry much of the load on the tail, as well as a transfer agent of the stresses back into the superstructure of the fuselage.

Fuselage shell – Fiberglass and carbon fiber materials were considered for the shell. While carbon fiber provides more strength than fiberglass, the fiberglass was ultimately chosen due to weight and budget concerns. A series of test shells were constructed to find the optimum number of layers of fiberglass to ensure that when subjected to minor loading and the dynamic pressure at flight velocities, the fiberglass would not deform from its aerodynamic shape. With the given sheet choice and the internal superstructure of the fuselage, it was found that only two layers of fiberglass were needed to ensure the rigidity of the skin during flight operations. The bottom of the fuselage was made in such a way that it could be removed to allow access into the cargo bay. To secure this section of fuselage to the top portion, basswood strips were placed on the fore and aft bulkheads, allowing secure attachments via small screws. Along the length of the fuselage more solid attachments will also be added in strategic sections to secure the payload hatch and ensure rigidity.

Landing gear – Both conventional and tricycle configurations were considered when selecting the landing gear. A conventional setup has the advantage that it saves on weight by introducing rear skids instead of a third wheel. A conventional setup also allows the wheels to be mounted on the structurally built up areas of the fore fuselage, allowing the structure of the aircraft to be somewhat concentrated there. Likewise, the conventional setup also allows for an initial angle of incidence while on the takeoff roll. The tricycle setup, however, has the advantage of taking possible ground looping out of play. Being that the pilot has experience with conventional gear in both calm and windy conditions, ground looping was considered a non-issue. Ultimately, a conventional setup was chosen. The gear strut was built of carbon fiber and to sit atop the fore bulkhead of the superstructure of the fuselage. Once attached, the landing gear spars extend outside of the plane and towards the front of the aircraft.

Rocket pylons – In order to attach the external payload to the wings an attachment system had to be devised. As removable pylons are permissible, the idea of having the pylon permanently attached to the rockets was chosen by the team for both simplicity of design as well as efficiency in materials. As such, the chosen design was to imbed an attachment point under the carbon fiber veneer on the underside of the wing. The rocket and pylon was then designed to be place up into the wing into the mount via a series of set screws.

5.3.2. Systems

Servos – Servos were chosen to be as light as possible, while still meeting the having the ability to exert sufficient torque on the control surfaces and the water drop system. The servos chosen were HITEC HS-65 servos for the ailerons, HITEC HS-85 for the tail surfaces, and HITEC HS-225MG servos for the flap. Being that these servos exert their maximum torques at low voltage levels (4.8 V), a small 4 cell battery was to be used for powering the control surfaces. The servo itself weighs only .9oz, and has dimensions of 0.9 x 0.4 x 0.8” allowing it to be discretely tucked away within the mold lines of the plane.

Flap Actuator – In order to move the flap from takeoff to cruise configuration, a system was designed with the goals of keeping weight and space occupied to a minimum. A Mystery SDS-SO307 servo was used to complete a circuit to a small motor attached to a threaded rod. The threaded rod carries the flap spars, guided by tracks in the fuselage, through their whole range of motion, and the flap position switch on the transmitter controls the whole system.

Receiver – As a composite material for the fuselage was not decided on until late in the design process, the receiver that was chosen was the Spektrum™ AR6255 6-Channel DSMX Carbon Fuselage Receiver.

The carbon compatible receiver is a must if a carbon fiber fuselage is to be used as carbon fiber is a conducting material, and thus the Faraday's cage effect must be considered. The carbon fuselage receiver thwarts this effect, and was so chosen allowing the team to choose a carbon fiber fuselage if it was seen as fit. Additionally, this receiver is a lightweight and compact package while still maintaining full range capabilities. The DSMX technology allows the receiver to be operated in the 2.4GHz band in close proximity to other aircraft on the same band, selecting separate channels to operate automatically to avoid interference or "lock out". As this receiver is a 6-Channel receiver, it is fully capable of handling the required number of channels that the design requires.

Batteries – As the power output of the batteries is directly proportional to the voltage placed across the motors, it was decided to create 10 cell NiMH battery packs made with Elite 1500 mAh cells. Given that the servos and receiver only call for an operating voltage of 4.8V, a smaller 4 cell NiMH battery was chosen for the receiver pack.

Speed controller – The motors chosen were of the brushless type, with a limited current of 20A. As such, a brushless speed controller rated at greater than 20A was sought. Two E-flite 25-Amp Airplane Brushless ESC's were ultimately chosen. Despite the fact that the motor could potentially draw over 20A for brief periods of time, it was assumed that the 25A speed controller could withstand the higher current without burning out given the rated amperage level, as well as the fact that the circuit would be protected with a 20A fuse.

Table 5.5. Control System Component Summary

Component Name	Component Description
HITEC HS-65	Aileron servo
HITEC HS-85	Tail servo
HITEC HS-225MG	Flap servo
Spektrum™ AR6255 6-Channel DSMX Carbon Fuselage Receiver	Receiver
4 Cell KAN 400 2/3AAA NiMH	Receiver Battery Pack
E-flite 25-Amp Airplane Brushless ESC	Speed Controller

Table 5.6. Control System Component Specifications

Servo	Weight [oz]	Torque @ 4.8V [oz-in]	Speed @ 4.8V [s/60°]
HITEC HS-55	0.6	36	0.11
HITEC HS-65	0.39	25	0.14
HITEC HS-81	0.67	41.66	0.16
HITEC HS-85	0.3	15	0.17
HITEC HS-225MG	1.09	54.15	0.14
S3114	0.27	21	0.1

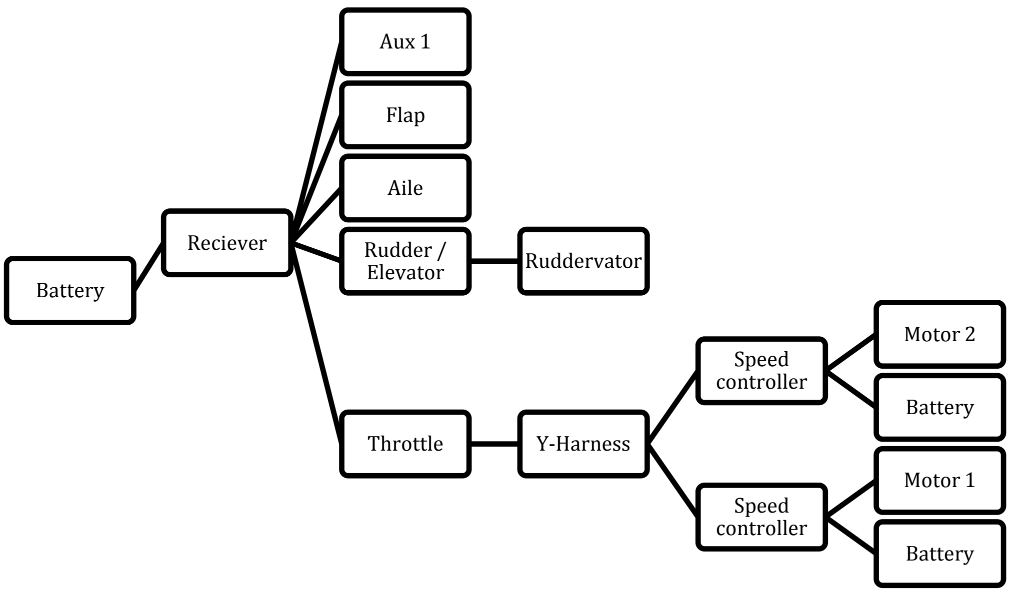

Fig. 5.1. Systems Circuit Flow-Chart

5.4 Weight and Balance

The weight and balance tables were based on component weights and distance from the leading edge of the wing, which served as a datum. The battery location was adjusted to keep the CG consistent in each mission. For the following table, the x-axis corresponds to the longitudinal axis, y-axis corresponds to the lateral axis, and z-axis corresponds to the yaw axis.

Table 5.7. Weight and Balance

Empty	Weight (lb)	CG location (in)	
		x	y
Airframe	2.20	0	19.1 – 20.9
Motor	.352	9 and -9	11.75
Propeller	0.011	9 and -9	10.75
Tail Servos	0.084	2 and -2	43.25
Aileron Servos	0.049	17.25 and -17.25	23.5
Radio receiver	0.011	0	38
Total	2.71	0	19.3

Table 5.8. Weight and Balance, Mission 1

Mission 1	Weight (lb)	CG Location (in)	
		x	y
Aircraft Empty	2.71	0	19.29
Batteries	1.0	3.5 and -3.5	18.5
Total	3.71	0	19.07

Table 5.9. Weight and Balance, Mission 2

Mission 2	Weight (lb)	CG Location (in)	
		x	y
Aircraft Empty	2.71	0	19.29
Batteries	1	3.5 and -3.5	14.5
Front Rockets	1	0	7.07
Rear Rockets	1	0	27.19
Total	5.71	0	19.08

Table 5.10. Weight and Balance, Mission 3

Mission 3 Option 1	Weight (lb)	CG Location (in)	
		x	y
Aircraft Empty	2.71	0	19.29
Batteries	1.00	3.5 and -3.5	17
Front rockets	0	0	0
Rear Rockets	1	0	28.5
Left Rockets	1	4.75	15
Right Rockets	1	-4.75	15
Total	6.71	0	19.04

Mission 3 Option 2	Weight (lb)	CG Location (in)	
		x	y
Aircraft Empty	2.71	0	19.29
Batteries	1.00	3.5 and -3.5	30.5
Front rockets	0	0	0
Rear Rockets	0	0	0
Left Rockets	1.5	4.75	15
Right Rockets	1.5	-4.75	15
Total	6.71	0	19.04

Mission 3 Option 3	Weight (lb)	CG Location (in)	
		x	y
Aircraft Empty	2.71	0	19.29
Batteries	1.00	3.5 and -3.5	24
Front rockets	0	0	0
Rear Rockets	0.5	0	28.5
Left Rockets	1	4.75	15
Right Rockets	1.5	-4.75	15
Total	6.71	-0.35	19.07

Mission 3 Option 4	Weight (lb)	CG Location (in)	
		x	y
Aircraft Empty	2.71	0	19.29
Batteries	1.00	3.5 and -3.5	30.75
Front rockets	0	0	0
Rear Rockets	0	0	0
Left Rockets	1.5	4.75	15
Right Rockets	1.5	-4.75	15
Total	6.71	0	19.07

Mission 3 Option 5	Weight (lb)	CG Location (in)	
		x	y
Aircraft Empty	2.71	0	19.29
Batteries	1.00	3.5 and -3.5	30.75
Front rockets	0	0	0
Rear Rockets	0	0	0
Left Rockets	1.5	4.75	15
Right Rockets	1.5	-4.75	15
Total	6.71	0	19.07

Mission 3 Option 6	Weight (lb)	CG Location (in)	
		x	y
Aircraft Empty	2.71	0	19.29
Batteries	1.00	3.5 and -3.5	27.25
Front rockets	0	0	0
Rear Rockets	0.25	0	28.5
Left Rockets	1.5	4.75	15
Right Rockets	1.25	-4.75	15
Total	6.71	0.18	19.06

5.5 Drawing Package

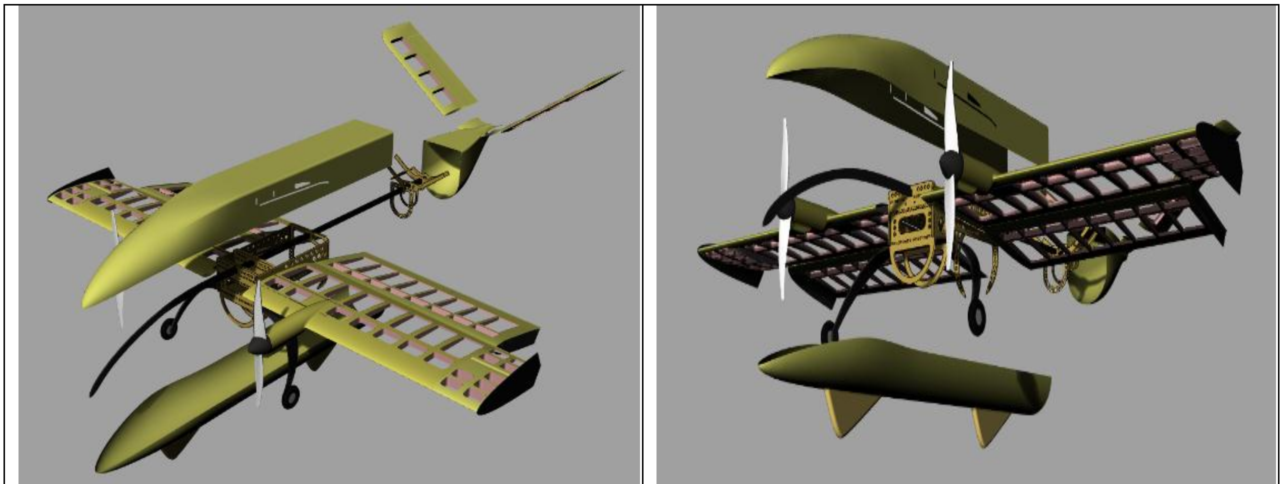

(a)	(b)

Fig. 5.1. (a) Top exploded perspective view; (b) Bottom exploded perspective view.

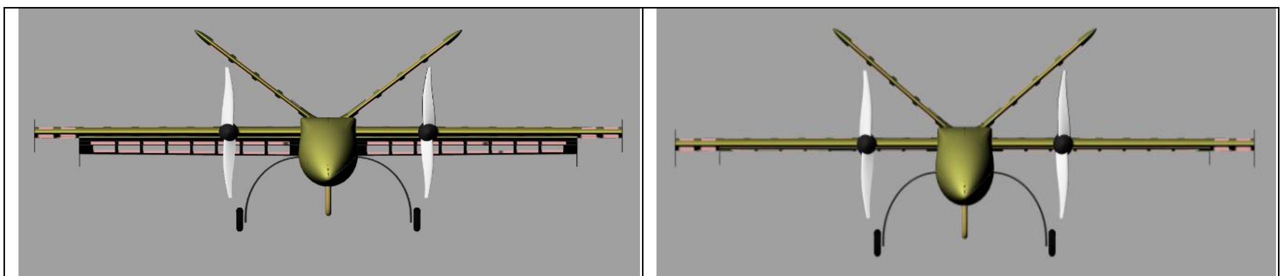

(a)	(b)

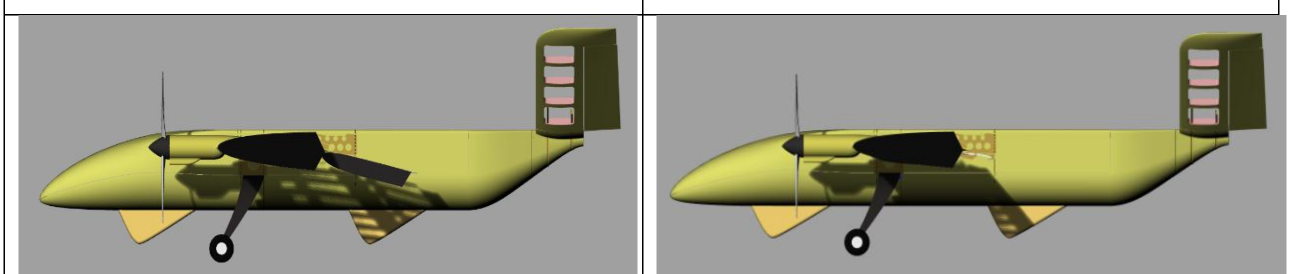

(c)	(d)

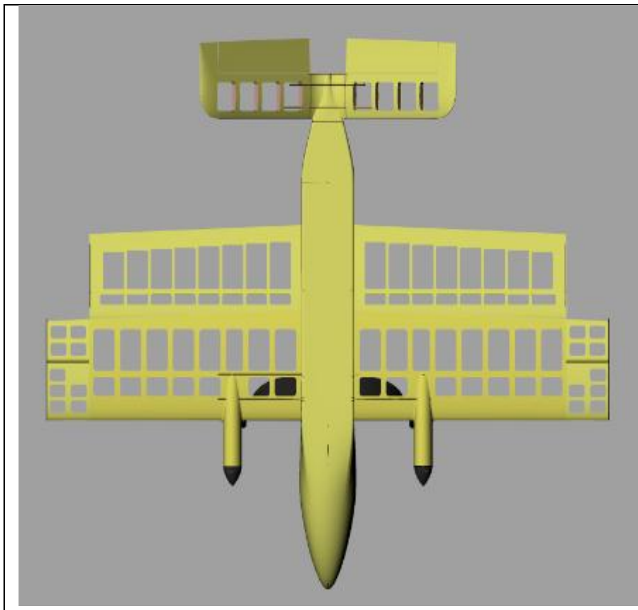	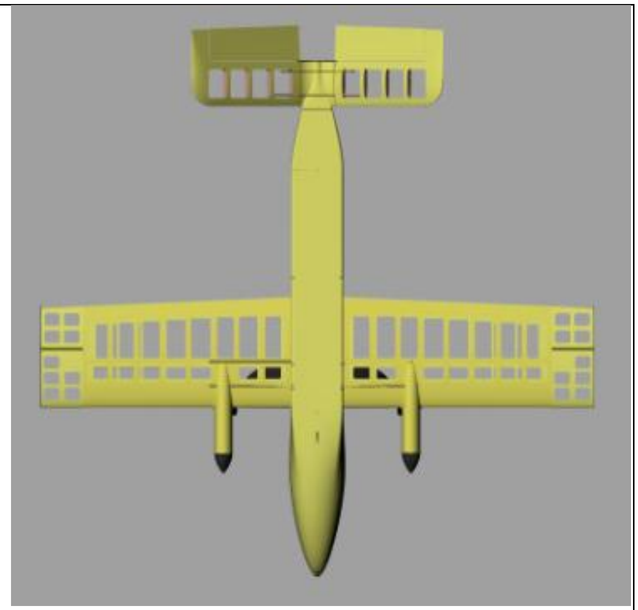
(e)	**(f)**

Fig. 5.2. (a) Front view, flaps deployed; (b) Front view, clean; (c) Side view, flaps deployed; (d) Side view, clean; (e) Top view, flaps deployed; (f) Top view, clean.

6. MANUFACTURING PLAN AND PROCESSES

6.1 Production Plan and Schedule

The manufacturing process included the construction of the three different models of the plane. First, the wind tunnel model was created, for which its main purpose was to be aerodynamically accurate. The wind tunnel model would be tested in University of Washington's Aeronautical Laboratory. Flight test model would be constructed capable of performing all three missions. The flight test model would be consistently modified to determine the best configuration for best performance. The competition model would represent the culmination of all that was learned from the previous iterations.

Before construction of the aircraft began, all parameters were assigned a score between 1 and 5, 1 being the worse and 5 the best. Following are the parameters considered:

- Weight – The relative weight a particular construction technique or method adds to the total weight of the plane. Lower weight gets higher score.
- Strength – The ability of a component or material to absorb forces acting on it without significant damage. This parameter is more important for some components than others. Higher strength gets a higher score.
- Simplicity – Simplicity includes the process of constructing and the time it takes to construct a component. Experience of the team with each construction technique is also taken into account. Higher simplicity gets a higher score.
- Cost – Cost was an unfortunate parameter that needed to be included due to budget limitations. Cheaper techniques and methods were preferred but were not always the deciding factor. Lower cost gets a higher score.

  Trait studies were conducted on every major component of the aircraft. Results are shown in Tables 30-32.

Table 6.2. Wing Construction Trade Study

Figures of merit	Balsa build up	Foam core w/ plywood coating	Foam core with carbon fiber coating	Carbon D-tube with ribs
Weight	5	4	2	3
Strength	3	2	5	4
Simplicity	3	5	4	1
Cost	4	5	3	1
Total	15	16	14	9

Table 6.3. Fuselage Construction Trade Study

Figures of merit	Balsa build up w/ plywood coating	Carbon fiber shell w/ ribs	Hollowed out foam
Weight	4	5	4
Strength	3	5	2
Drag	3	5	4
Simplicity	3	2	2
Cost	4	4	3
Total	17	21	15

Table 6.4. Tail Construction Trade Study

Figures of merit	Balsa build up	Foam core w/ plywood coating	Foam core with carbon fiber coating
Weight	5	3	4
Strength	3	4	5
Simplicity	3	5	4
Cost	4	5	3
Total	15	17	16

From the trade study, the winning building method for the wing and tail was foam core with a plywood veneer, and for the fuselage a carbon shell with ribs. While these were the results from the trade study, the actual building methods deviated, with all parts moving to carbon fiber veneered foam cores. The reason behind doing this was two-fold: the complexity was negated by already having to go through the molding process for the carbon fiber layups for the fuselage, and also to retain the uniformity of stress distribution through the junctions of the wings, tail, and fuselage.

With the building techniques finalized it was possible to come up with a manufacturing schedule as shown in Fig. 6.1.

	December					January				February				March				
Task	1-	8-	15-	22-	29-	5-	12-	19-	26-	2-	9-	16-	23-	1-	8-	15-	22-	29-
Wind Tunnel Model																		
Wings																		
Carbon Fiber																		
Fuselage																		
Tail																		
Servos and Wiring																		
Flight Test Model																		

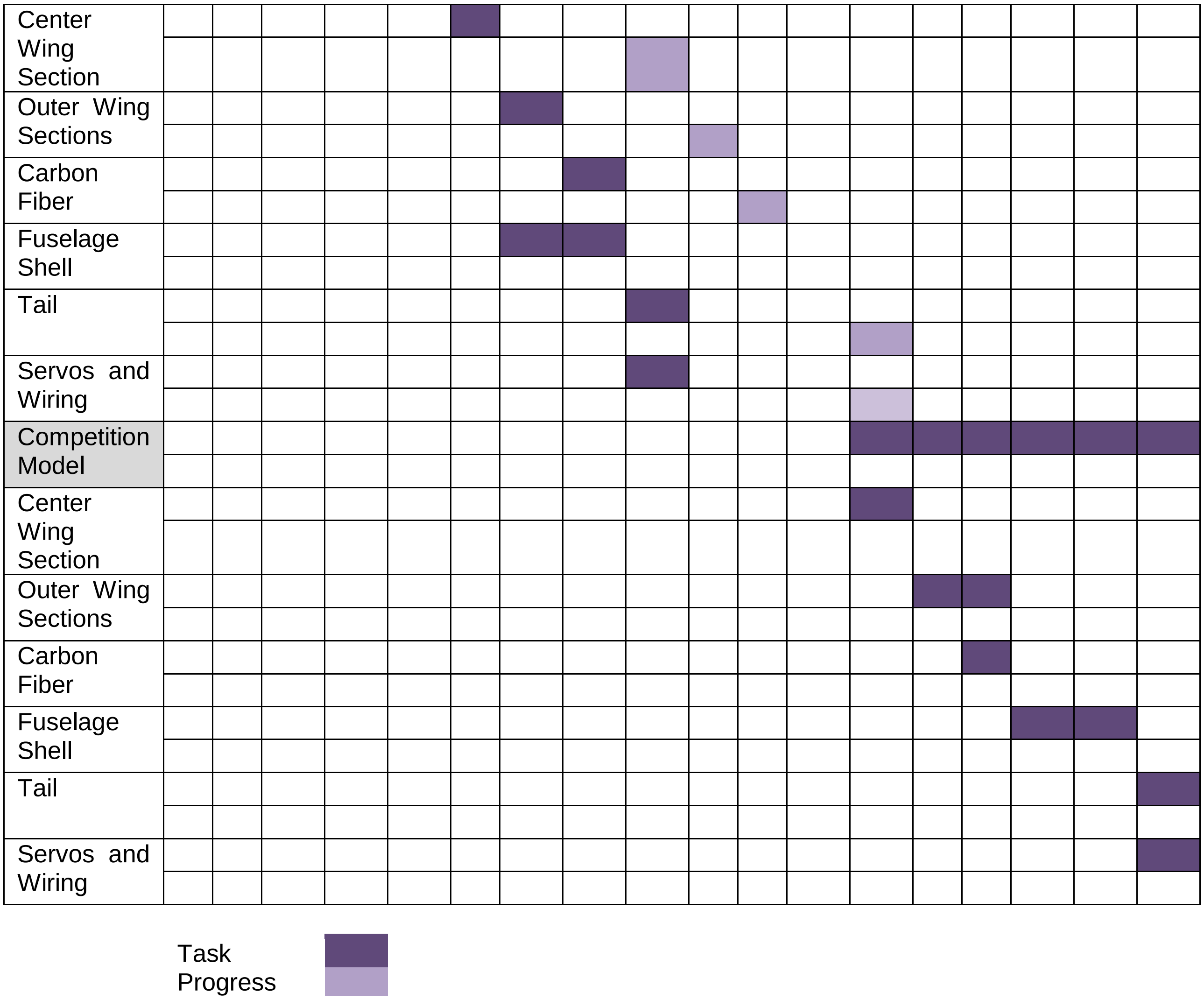

Fig. 6.1. Manufacturing Timeline

6.2 Manufacturing Process

The manufacturing process was broken up into three distinct areas: fuselage, wings, and empennage.

6.2.1. Fuselage

The fuselage has two major components: the fiberglass shell and the internal superstructure. All of the superstructure and flap structure components were laser cut from 1/8th inch model grade plywood with the exception of carbon fiber spars.

For the manufacturing of the fiberglass shell, SolidsWorks parametric modeler was used to create surface molding files which were subsequently milled using a 3-axis mill. The molds were modeled using the female mold vacuum single-sided vacuum bagging technique, with the surfaces corresponding to the port and starboard sections of the fuselage. The chosen fiberglass cloth was a lightweight cloth. As the fuselage does not bear any direct loads, it does not need to maintain the same level of structural integrity as the rest of the fuselage sections. Likewise, with the fiberglass shell being supported by the internal superstructure, it was able to be optimized for aerodynamic accuracy and low weight.

The superstructure was designed not only to maintain structural integrity throughout the fuselage connection points (i.e., wing attachment and tail attachment points), but also to support the flap structure and internal payload, as well as maintain the aerodynamic shape for the fiberglass. The main support structure within the superstructure comes in the form of a 1 cm by 1 cm hollow square carbon spar that runs parallel to the flight axis of the aircraft. This spar was chosen for its rigidity to bending loads, adequate torsional characteristics, and the ease of mounting substructures to a square spar as opposed to a circular spar. Attached to the spar are two bulkheads, one at the leading edge of the wing, and one at the trailing edge of the fully extended flap. Connecting the bulk heads is both the carbon spar as well as two rectangular support pieces. Within the rectangular support pieces are hard-point connections for the wing roots as well as track for the flap spar to travel within. Atop the forward bulkhead sits the electronic components of the flap extension system. Behind the aft bulkhead the tail support attaches to the carbon spar through more laser cut plywood.

6.2.2. Wings

The wings were manufactured from foam cut panels laminated in carbon fiber. The panels were cut using airfoil profiles and hot-wires guided by stainless steel stencils created in the shape of the desired airfoil. Since the design called for a wing that would hold the shape of one airfoil while in the cruise configuration and then morph into the shape of a different highly cambered airfoil in the takeoff configuration, the flap would have to be cut out of the shape of the cruising airfoil. As such, the foam cores were cut in the shape of the cruising airfoil, from which the flap panels were also wire cut. The foam cores for the wings only needed to be able to keep the aerodynamic shape as well as take the shear loading within the wings.

Essentially, the wings were built based on the model of a shear wall. As such, it was possible to mill out unnecessary material from the foam cores of the wings and aileron sections using a foam CNC machine. Likewise, it was possible to use the foam CNC machine to mill out channels for the wires to the servos and the carbon spars, as well as cavities for the servos to sit within. With the milling done, the foam cores were then able to be veneered with the carbon fiber sheeting.

Within the flaps there are two imbedded carbon spars inboard, with the fore spar running through and into a flap track placed between inboard of the flap, within the wire cut foam. With the foam cut and the spar channels milled, the flap sections were then covered with carbon fiber sheeting.

6.2.3. Empennage

Like the main wings, the surfaces comprising the tail were formed from foam surfaces. These foam cores, however, were milled from the blanks as opposed to being wire cut. For this section, the carbon sheeting was more complex than that of the other sections. To fair the V-tail design into the fuselage and maintain full range of motion of the control surfaces, the carbon fiber sections for the aft fuselage and the tail were made into one piece. The mold was split into two about the top and bottom of the fuselage. In doing this, it was possible to mold the top part of the fuselage – tail connection with part of the tail airfoil into it. This allowed for the tail to be faired into the fuselage, and allowed for the structure of the tail to be better worked into the superstructure of the fuselage.

7. TESTING PLAN

7.1 Objectives

7.1.1. Wind Tunnel Testing

Within the same building that UW DBF operates happens to be the largest student run wind tunnel in the United States, the Kirsten Wind Tunnel. With several students employed there, the team had access to extensive wind tunnel testing. The first prototype, which has been referred to as the wind tunnel model, was built with special hard-points to allow it to be mounted within the wind tunnel. With the wind tunnel model, it was decided to do tail-off testing. The reasoning behind this was that a tail off test would allow for the tail to be designed specifically to offset the pitching moments seen from the wing-body combination, in each of its forms. This was seen to be a better testing method than to place an arbitrary tail onto the plane, as one had yet to be designed.

To attempt to simulate the drag seen from the tail during the testing, two circular carbon fiber booms were placed in the approximate location of the tail, at the approximate dihedral. Circular sections were chosen as they will create more drag than an airfoil shape of the same size. With a full authority balance, the model was capable of being pitched and yawed to any combination of angle desired during testing. Variations of dynamic pressure, angle of attack, yaw angle, and control surface settings would result in measurements of roll and tail moments, lift, and drag. These measurements were necessary to be able to calculate the lift, drag, and moment coefficients of the aircraft. Having the physical data from the wind tunnel testing allowed for variations to be made to the design to improve efficiency, correct sizing issues for either the tail or the main wings, determine the aerodynamic center of the wing-body combination, and locate the necessary center of gravity location.

7.1.2. Structural Tests

Structural tests were performed on main components of the plane to verify their structural integrity. The wings were first tested within SoldiWorks' SimulationXpress simulation tool. Figure 7.1 shows the landing gear strut, made of 1/8th inch carbon sheeting under an approximated maximum loading condition. Looking at the Von Mises, the stress concentrations could be visualized, noting the likely points of failure of the spar. From SimulationXpress, the minimum factor of safety for the landing gear spar was found to be 40, allowing for the part to be significantly optimized.

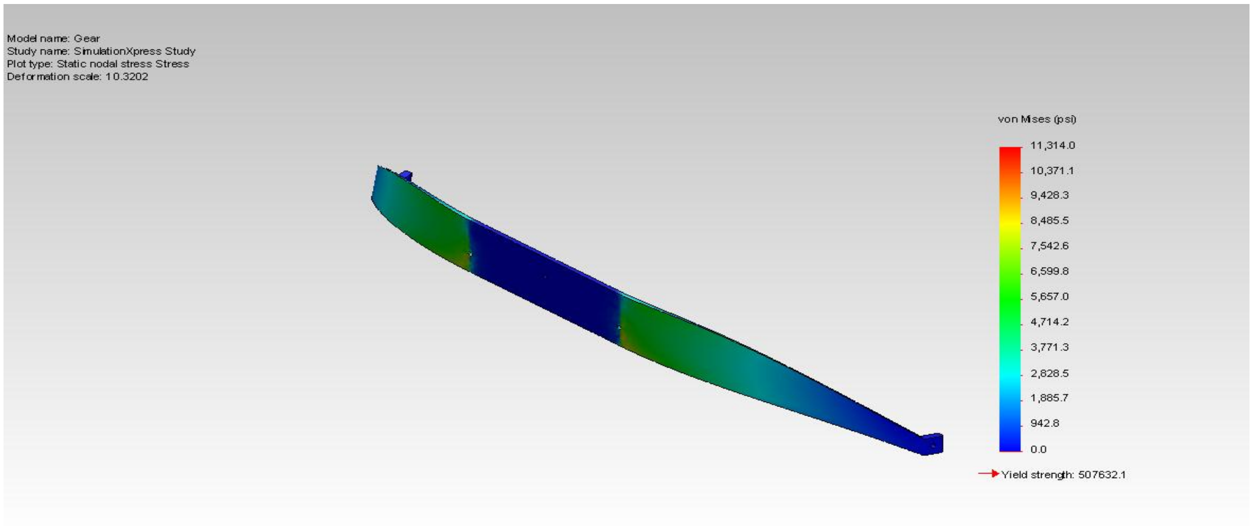

Fig. 7.1. Von Mises stress concentrations on landing gear strut.

Likewise, simulations were run with various loadings applied on the wing model to determine the stress concentration areas of the wing. Again from SimulationXpress, the Von Mises stresses could be visualized, as shown in Fig. 7.2, and the factor of safety of the carbon spar of the wing was found to be 70. While the spar itself was over-engineered, the simulation did not take into account the fact that the wing is a composite body made up of the carbon spar, the foam core, and the carbon veneer. The carbon components of the wing were also tested using two table vises, placing bending loads on the carbon structure to ensure that they would be able to withstand the maximum estimated loads (twice the weight of the aircraft).

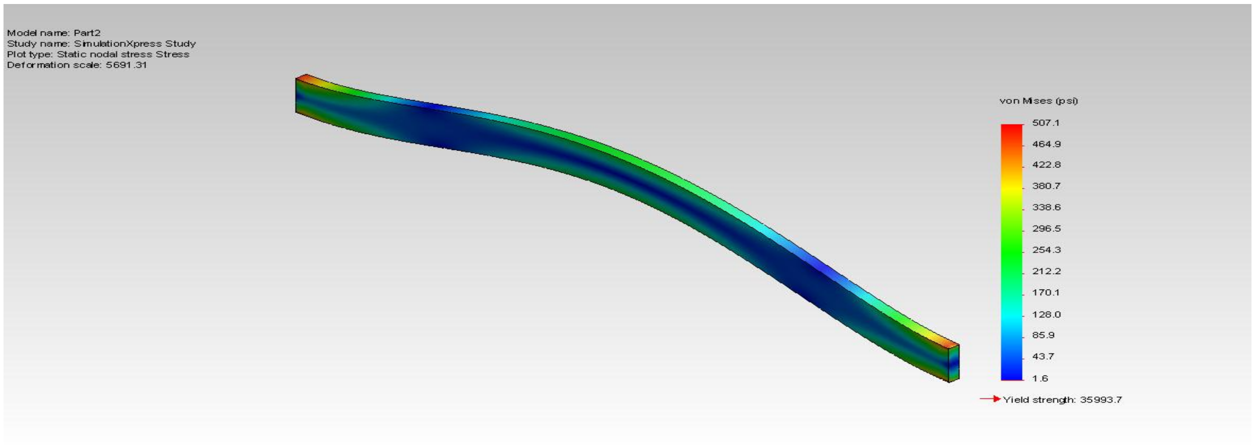

Fig. 7.2. Von Mises stress concentration on wing spar.

7.1.3. Propulsion Tests

For the purposes of propulsion testing, the University of Washington's 3x3 foot wing tunnel was utilized. The purpose of this testing was to find the potential motor and propeller combinations that would give the best results through the widest range of operating conditions for the aircraft and the given missions. By testing the motors and propellers in the wind tunnel, it was possible to find the efficiencies of the motor

8. PERFORMANCE RESULTS

Following the results of the wind tunnel test, there was a period of several weeks while materials for a flight test model were accumulated and the final design process was finished. Following the construction and assembly of the flight test model, a flight test was carried out at Magnuson Park in Seattle, Washington.

8.1 Electrical Systems Performance

All control systems functioned correctly, and the flap actuation system worked properly, providing slow, steady movement of the flaps. The 20 amp fuse was blown in several of the initial takeoff attempts, but after the correct throttle limit was programmed into the transmitter, this was no longer an issue. The battery packs used were each 10-cell units, but this number may be modified to suit each mission profile.

8.2 Total Aircraft Performance

On the first successful takeoff, the airplane was too “nose-heavy” in its handling characteristics, and so internal loading and trim were changed to produce a more neutral feel. Of the first 20 takeoffs, 13 successfully occurred within the 30’ x 30’ box. 4 of the failed attempts were due to adverse wind conditions, and 3 were due to a lack of power from overly discharged battery cells. Based on these results, it is likely that the airplane will require design alterations in order to ensure that a successful takeoff can happen even in poor wind conditions. The airplane demonstrated high cruise speed and good maneuverability, even when carrying the maximum load.

REFERENCES

[1] AIAA, "2012/13 Rules and Vehicle Design", October 2012. Accessed 9/25/12. [http://www.aiaadbf.org/2013_files/2013_rules.htm]

[2] Raymer, Daniel P. *Aircraft Design : A Conceptual Approach*. Reston, VA: American Institute of Aeronautics and Astronautics, 1999. Print.